Electronic Supplementary Information

# Enhanced Thermoelectric Performance in $Mg_{3+x}Sb_{1.5}Bi_{0.49}Te_{0.01}$ via Engineering Microstructure through Melt-Centrifugation

Melis Ozen,[a,b] Mujde Yahyaoglu,[a,b] Christophe Candolfi,[c] Igor Veremchuk,[d] Felix Kaiser,[e] Ulrich Burkhardt,[e] G. Jeffrey Snyder,[f] Yuri Grin,[e] and Umut Aydemir*[b,g]

[a] Graduate School of Sciences and Engineering, Koç University, Istanbul-34450, Turkey

[b] Koç University Boron and Advanced Materials Application and Research Center, Istanbul-34450, Turkey

[c] Institut Jean Lamour, Université de Lorraine, Nancy Cedex-54011, France

[d] Helmholtz-Zentrum Dresden-Rossendorf, Institute of Ion Beam Physics and Materials Research, 01328 Dresden, Germany

[e] Max Planck Institute für Chemische Physik Fester Stoffe, Dresden-01187, Germany

[f] Department of Materials Science and Engineering, Northwestern University, Evanston, IL-60208, USA

[g] Department of Chemistry, Koç University, Sariyer, Istanbul, 34450, Turkey

Email: uaydemir@ku.edu.tr

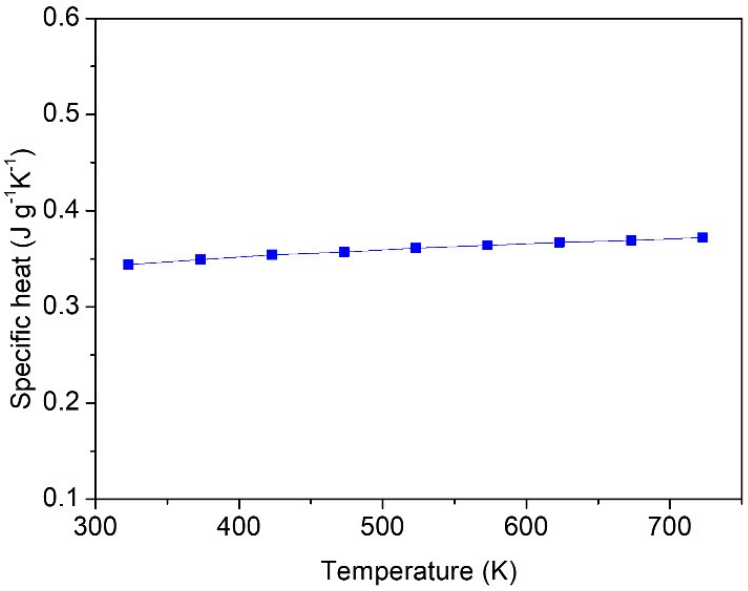


**Figure S1.** Specific heat of $Mg_{3.2}Sb_{1.5}Bi_{0.49}Te_{0.01}$ calculated by Maier-Kelley equation as a function of temperature[1, 2].

Fig. S2 shows the phase diagram of the Mg-Sb system. Because it contains eutectic points in two different two-phase regions (Mg-$Mg_3Sb_2$ and $Mg_3Sb_2$-Sb), the melt centrifugation technique is applicable to both Mg-excess and Sb-excess compositions. As seen from the diagram on the left side of $Mg_3Sb_2$ (as marked by the vertical red dotted lines in the figure), a mixture of Mg and $Mg_3Sb_2$ can be acquired through adding an excess amount of Mg. By subsequent heat treatment of the mixture at a temperature higher than the eutectic point (627°C), but lower than the melting point of the main $Mg_3Sb_2$ phase, one can get a solid $Mg_3Sb_2$ phase with the liquid phase. In this sense, *n*-type $Mg_3Sb_2$ samples with porous microstructure and dislocation arrays can be obtained by the removal of liquid Mg with centrifugal force.

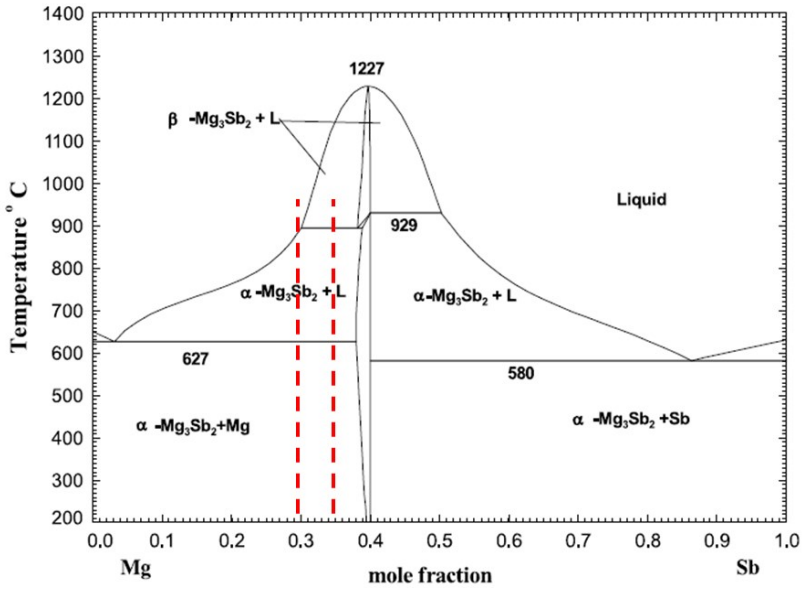


**Figure S2.** Binary phase diagram of Mg-Sb[3].

The lattice parameters of samples with starting compositions $Mg_{3.2}Sb_2$, $Mg_{3.2}Sb_{1.5}Bi_{0.49}Te_{0.01}$ and centrifuged $Mg_{3.2}Sb_{1.5}Bi_{0.49}Te_{0.01}$ samples were evaluated by using the WinCSD program (Table S1). An increase in the lattice parameters was observed by XRD phase analysis; implying successful incorporation of Bi and Te into the crystal structure of $Mg_3Sb_2$. What is more, extending the time of heat treatment (from 30 to 60 min) coupled with centrifugation, leads to even further increase in lattice parameters, suggesting a slight change in the chemical composition.

**Table S1.** Lattice parameters (a and c space group $P\bar{3}m1$, structure type $La_2O_3$) of samples investigated.

| Starting Composition | a (Å) | c(Å) |
|---|---|---|
| **$Mg_{3.2}Sb_2$** | 4.560(1) | 7.223(4) |
| **$Mg_{3.2}Sb_{1.5}Bi_{0.49}Te_{0.01}$** | 4.582(4) | 7.286(7) |
| **MSBT_20ext_30m_c** | 4.613(3) | 7.317(6) |
| **MSBT_20ext_1h_c** | 4.596(1) | 7.295(3) |

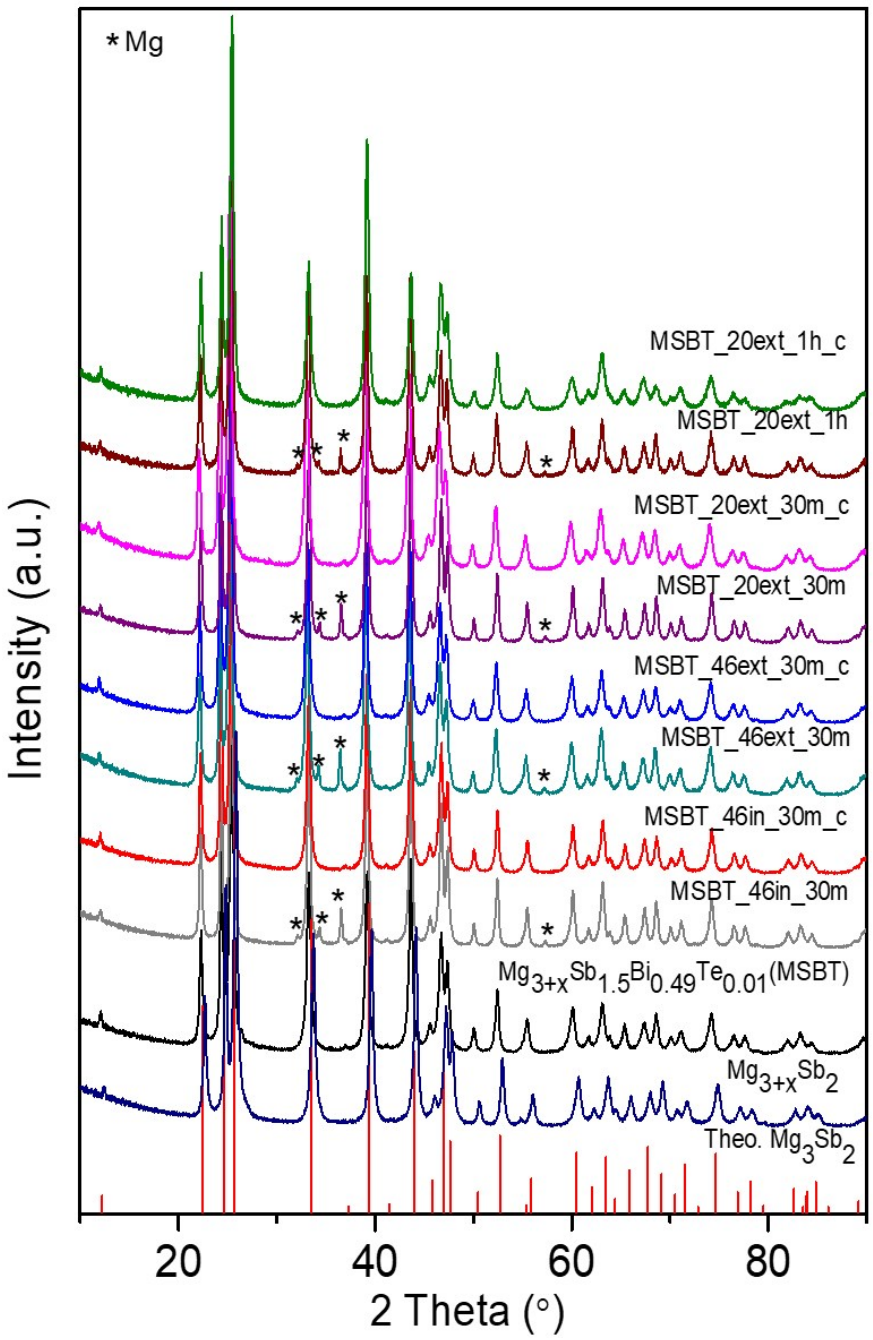


**Figure S3.** XRD patterns (Cu-$K_{\alpha 1}$ radiation) of parent $Mg_{3+x}Sb_2$, MSBT samples and centrifuged samples before and after centrifugation process

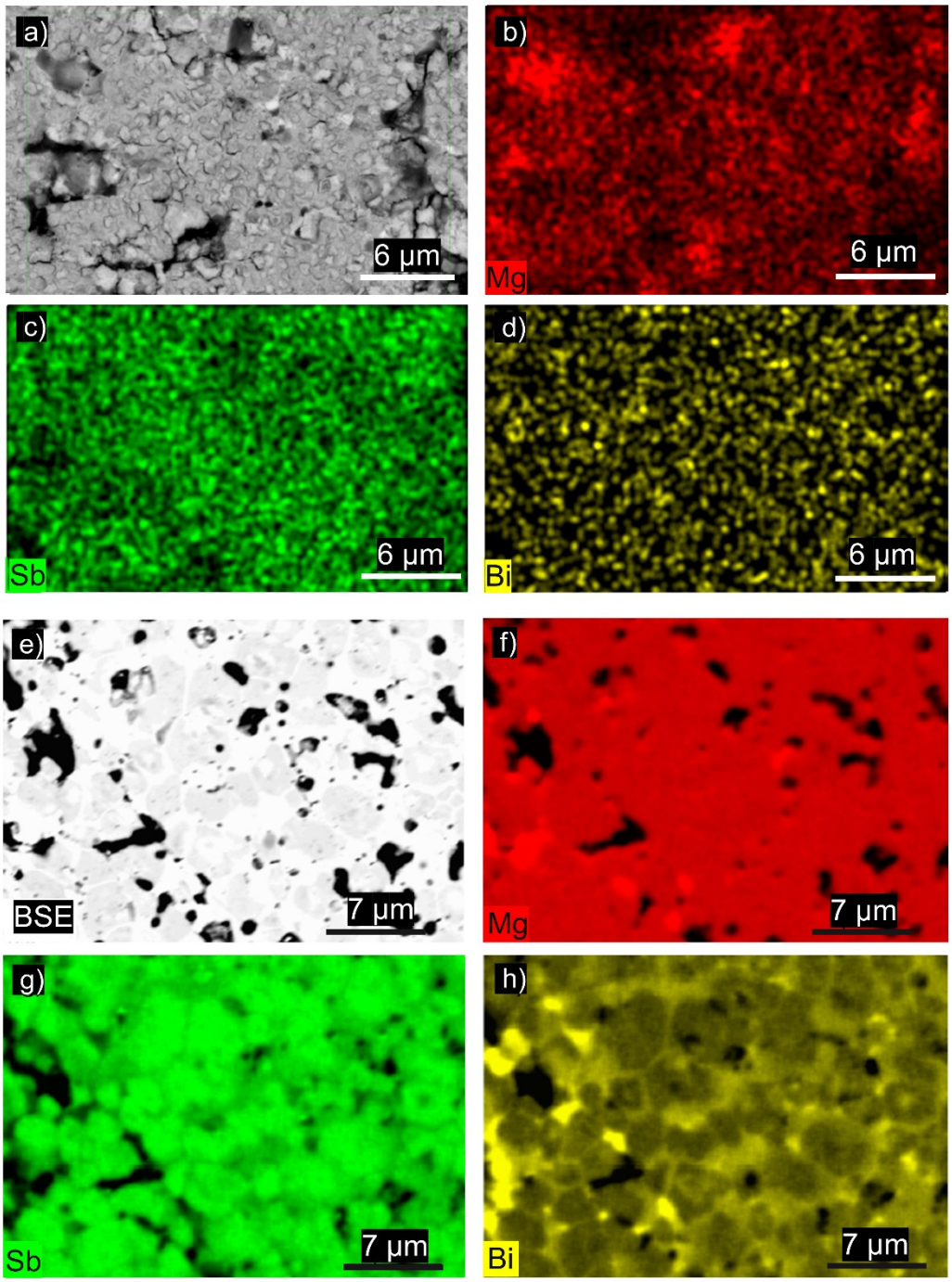


**Figure S4.** a) SE image (20.0 kV HV) of MSBT_20ext_1h_c sample with elemental mapping of b) Mg, c) Sb, d) Bi,and e) BSE image (10.0 kV HV) of MSBT_20ext_30m_c sample with elemental mapping of f) Mg, g) Sb, h) Bi.

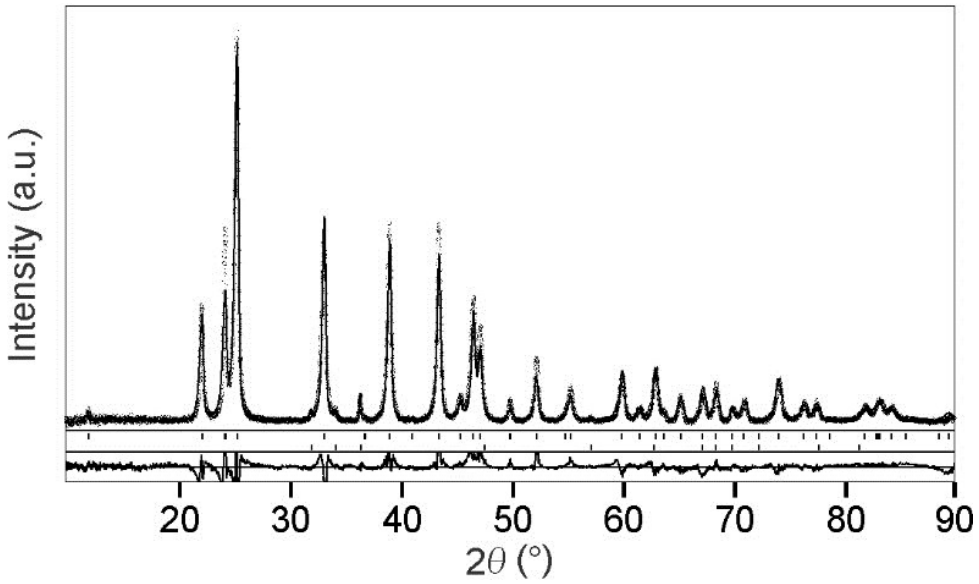


**Figure S5.** Rietveld fit of MSBT_20ext_1h (Cu-$K_{\alpha1}$ radiation). Ticks at the top and bottom mark the calculated reflection positions of the target phase $Mg_3Sb_2$ and Mg, respectively. The baseline corresponds to the residuals of a Rietveld refinement ($R_i$ = 0.06, $R_p$ = 0.14, $R_{wp}$ = 0.19) based on the reported crystal structure. In the crystal structure of $Mg_3Sb_2$ (space group: $P\bar{3}m1$), there are two Mg (1*a* and 2*d*) and one Sb (2*d*) Wyckoff sites. The refinement indicates that all the Mg sites are fully occupied, while the Sb site is mixed occupied (0.74(2) Sb and 0.26(2) Bi).

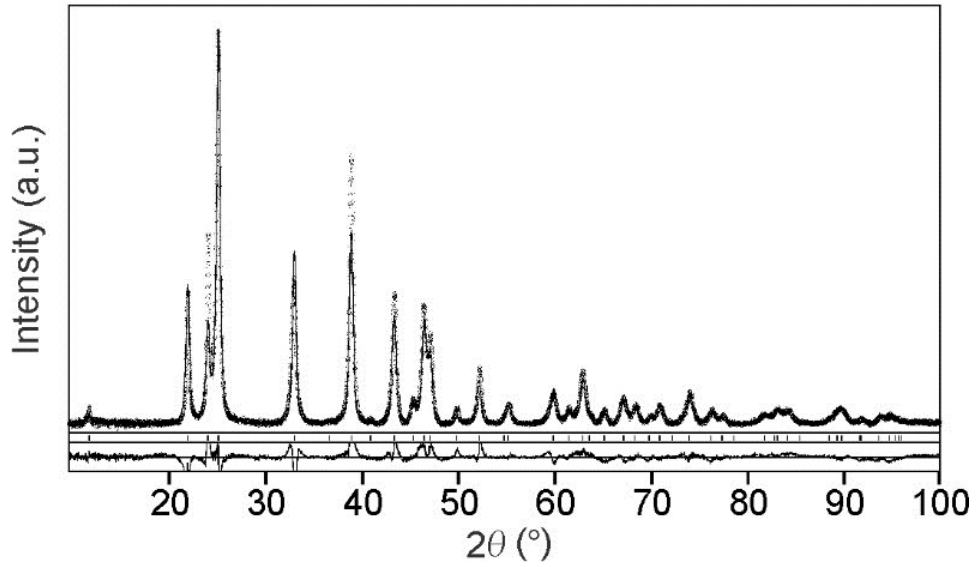


**Figure S6.** Rietveld fit of MSBT_20ext_1h_c (Cu-$K_{\alpha1}$ radiation). Ticks mark the calculated reflection positions of the target phase $Mg_3Sb_2$. The baseline corresponds to the residuals of a Rietveld refinement ($R_i$ = 0.08, $R_p$ = 0.16, $R_{wp}$ = 0.20) based on the reported crystal structure. In the crystal structure of $Mg_3Sb_2$ (space group: $P\bar{3}m1$), there are two Mg (1*a* and 2*d*) and one Sb (2*d*) Wyckoff sites. The refinement indicates that all the Mg sites are fully occupied, while the Sb site is mixed occupied (0.78(2) Sb and 0.22(2) Bi).

WDS analysis was carried out for MSBT sample on 10 different spots (Figure S7. and Table S2). For this, the composition of the sample was determined to be $Mg_{3.08(1)}Sb_{1.44(2)}Bi_{0.47(1)}Te_{0.01(3)}$, which is almost the same stoichiometry as the nominal composition.

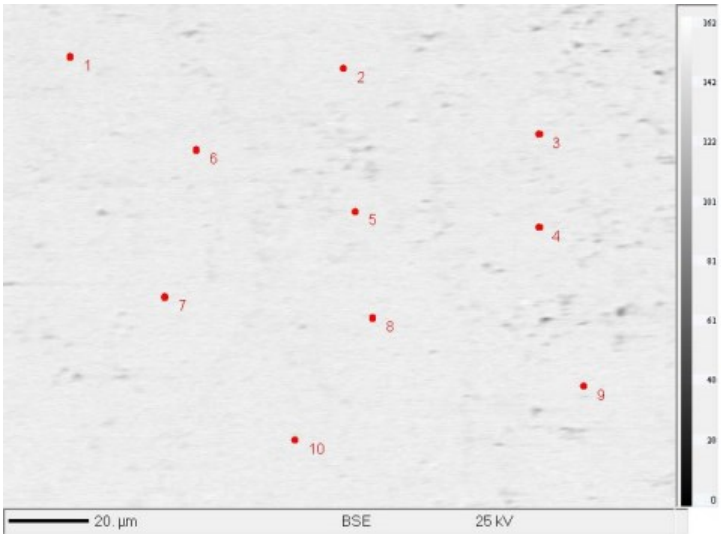


**Figure S7.** WDXS analysis of $Mg_{3+x}Sb_{1.5}Bi_{0.49}Te_{0.01}$ sample was performed on 10 different, randomly-chosen spots.

**Table S2.** WDS analysis results (average on 10 points) for the sample $Mg_{3+x}Sb_{1.5}Bi_{0.49}Te_{0.01}$.

| | Atomic Percent | Standard Deviation |
|---|---|---|
| **Mg** | 61,6 | 0,2 |
| **Sb** | 28,8 | 0,3 |
| **Bi** | 9,4 | 0,2 |
| **Te** | 0,221 | 0,006 |
| **Total** | 100 | |

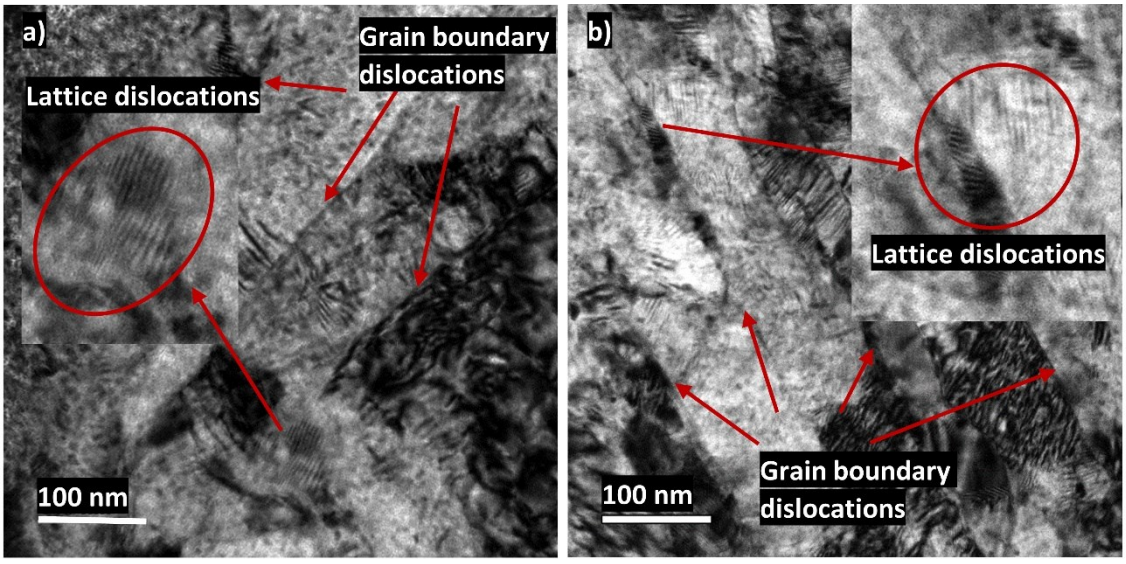


**Figure S8.** Bright Field TEM images of MSBT_20ext_30m_c taken from a) out-of-plane direction and b) in-plane direction.

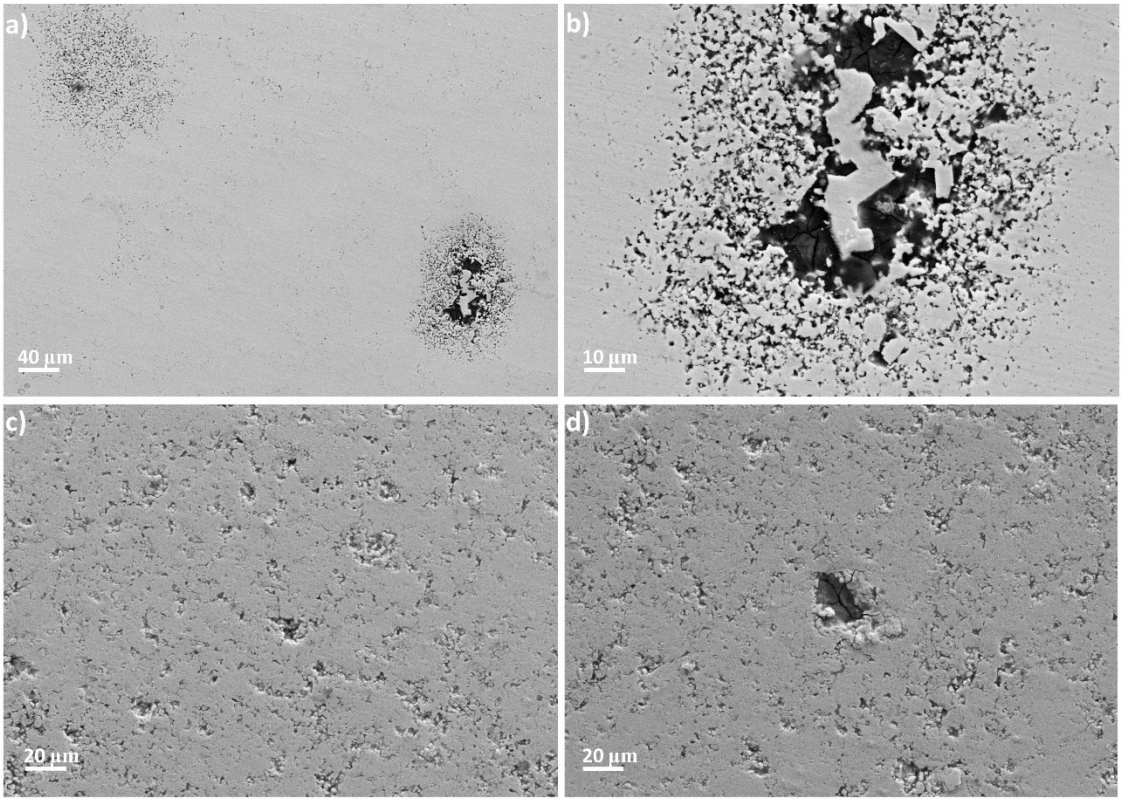


**Figure S9.** SEM images of MSBT_20ext_30m_c (a and b; 20.00 kV EHT) and MSBT_20ext_1h_c (c and d; 20.00 kV EHT) in secondary electron mode (SE).

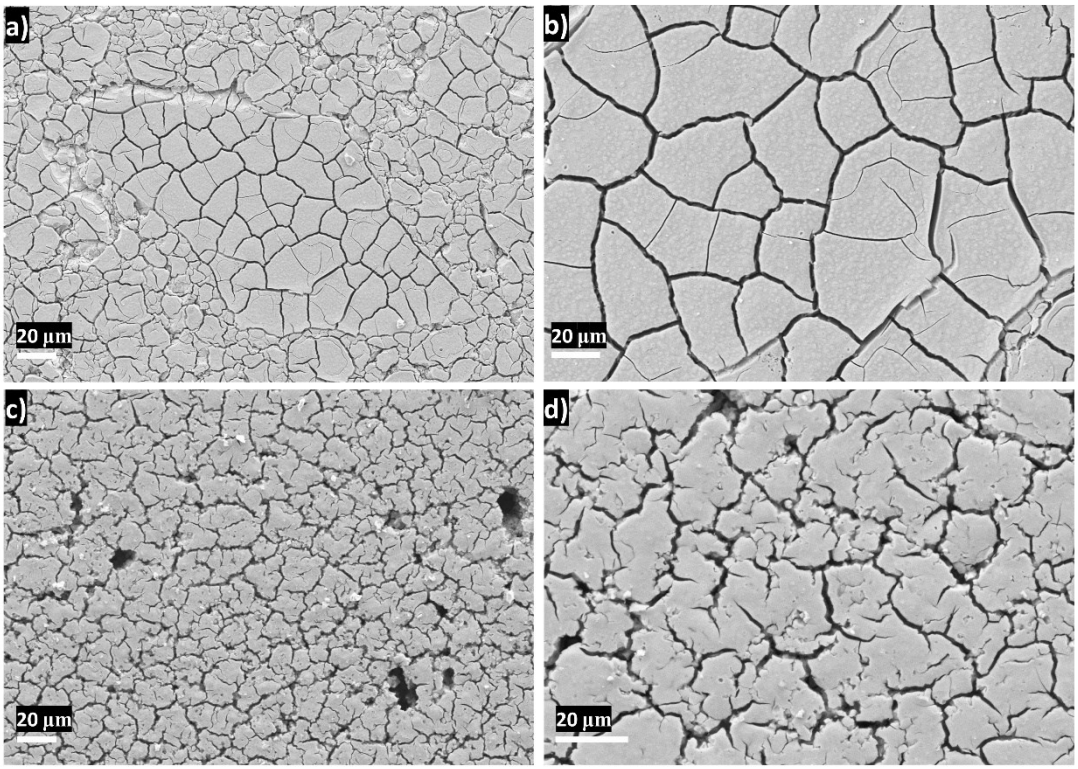


**Figure S10.** SEM images of MSBT_20ext_30m_c (a and b; 20.00 kV EHT) and MSBT_20ext_1h_c (c and d; 20.00 kV EHT) in secondary electron mode (SE) after etching process.

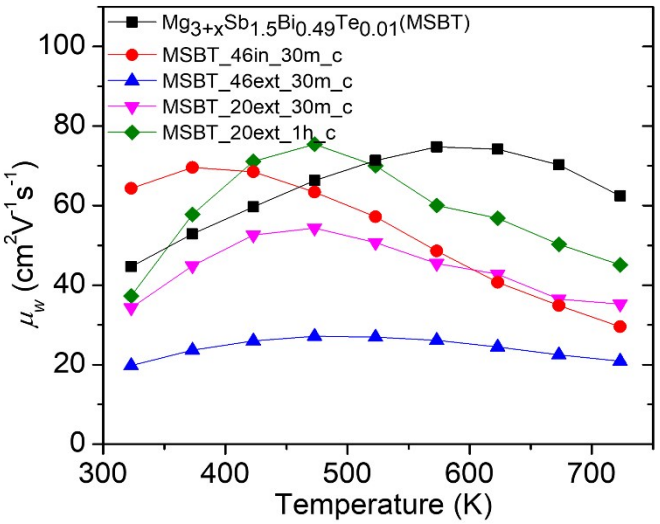


**Figure S11.** Calculated weighted mobility data of MSBT (black), MSBT_46in_30m_c (red), MSBT_46ext_30m_c (blue), MSBT_20ext_30m_c (pink) and MSBT_20ext_1h_c (green) as a function of temperature.

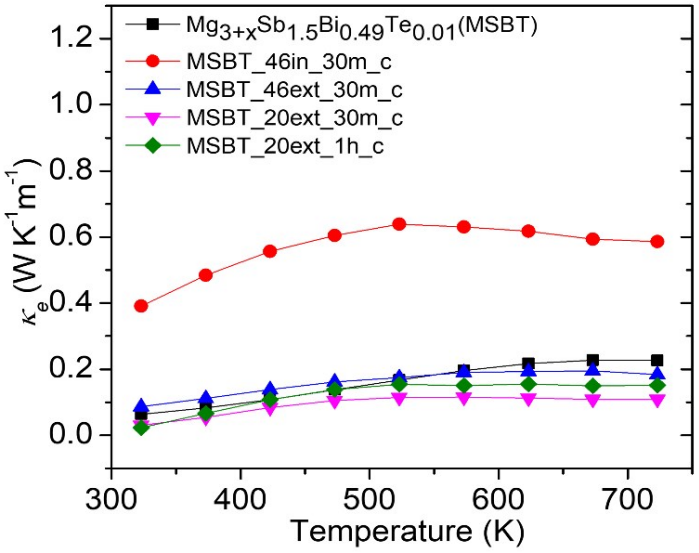


**Figure S12.** Temperature dependence of the electronic thermal conductivity $\kappa_e$ of MSBT (black), MSBT_46in_30m_c (red), MSBT_46ext_30m_c (blue), MSBT_20ext_30m_c (pink) and MSBT_20ext_1h_c (green) samples as a function of temperature.

**Table S3.** Densities and relative densities of spark plasma sintered and centrifuged samples calculated by the geometrical method.

| | MSBT | MSBT_46in_30m_c | MSBT_46ext_30m_c | MSBT_20ext_30m_c | MSBT_20ext_1h_c |
|---|---|---|---|---|---|
| **Density (g/cm$^3$)** | 4.3 | 3.27 | 3.35 | 3.89 | 3.83 |
| **Relative Density %** | 95.7 | 72.8 | 74.6 | 86.6 | 85.3 |

As seen in Table S3, the consolidated MSBT sample showed a high relative density of ~96%. Even though spark plasma sintering technique produced highly densified materials, centrifugation formed a porous microstructure.In this respect, after the centrifugation process, the relative densities were significantly reduced.

A glance at relative density values given in Table S3 disclose that relative density has a reverse relation with excess Mg, meaning that with increasing Mg excess amount relative density decreases. The induced porosities for the last two samples are shown in FigureS9.

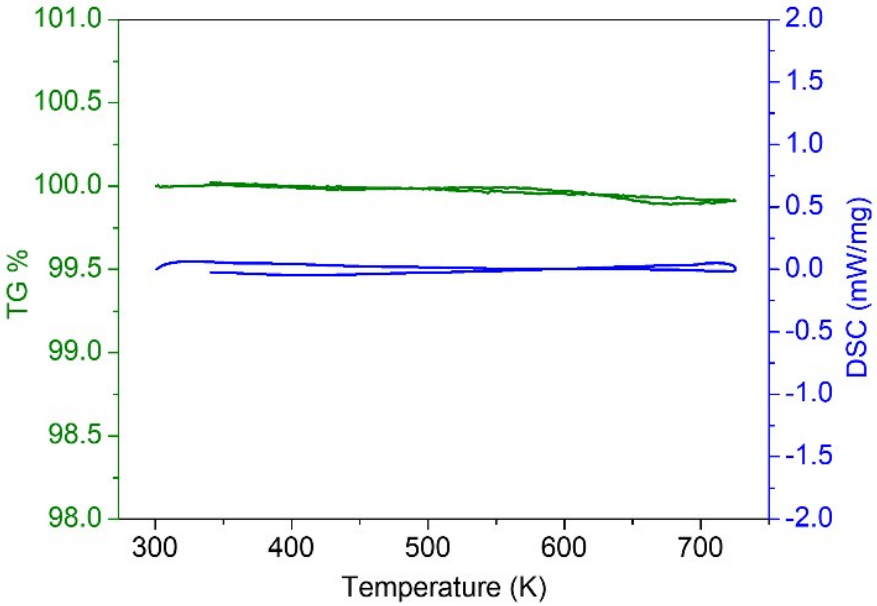


**Figure S13.** DSC/TG analysis of melt-centrifuged MSBT_20ext_30min_c sample.

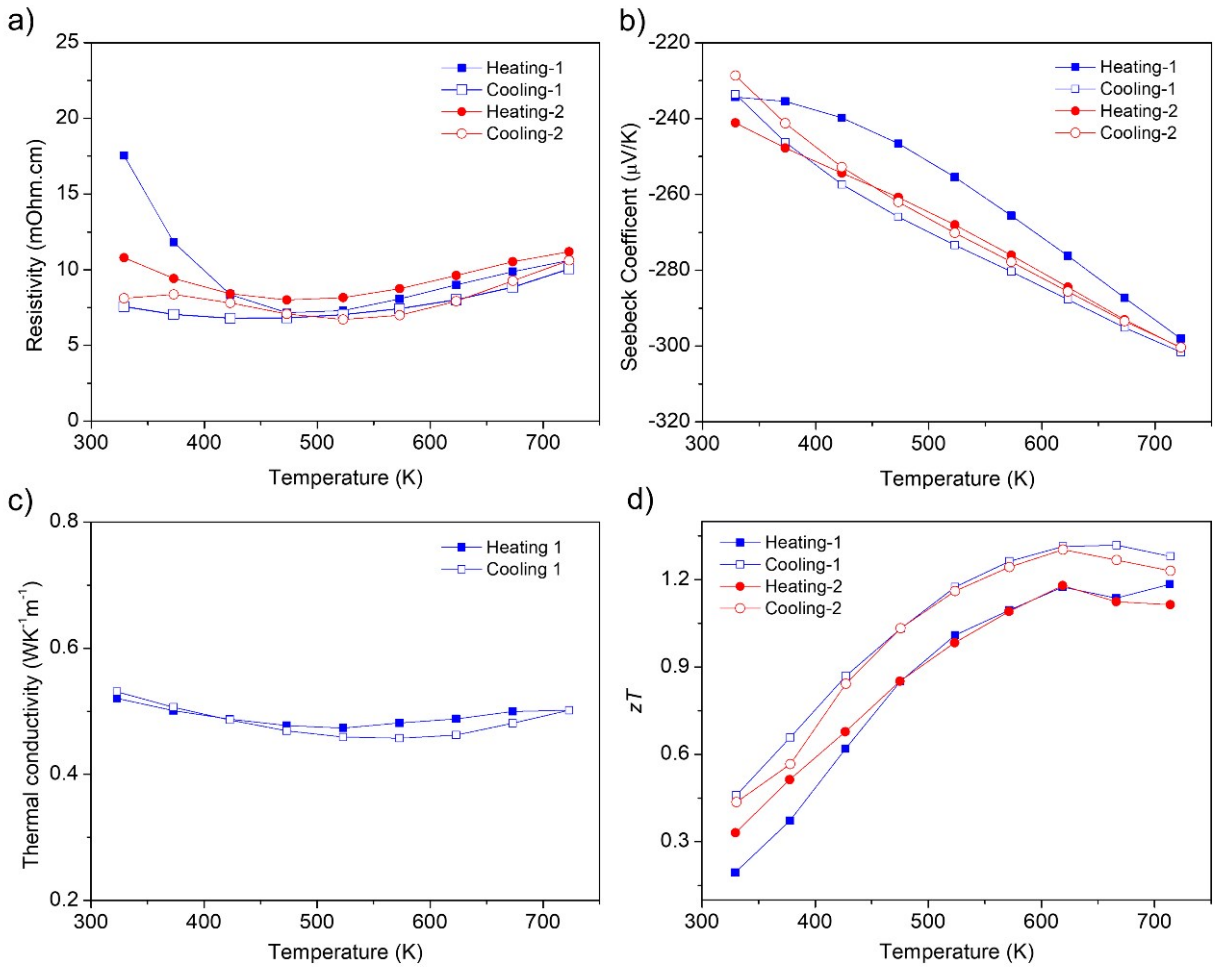


**Figure S14.** Temperature dependence of a) electrical resistivity, b) Seebeck coefficient, c) thermal conductivity and d) thermoelectric figure of merit *zT* values of MSBT_20ext_30m_c sample. The stability of melt-centrifuged sample is shown by heating-cooling cycles for the same sample.

**References**


1. M. T. Agne, K. Imasato, S. Anand, K. Lee, S. K. Bux, A. Zevalkink, A. J. Rettie, D. Y. Chung, M. G. Kanatzidis and G. J. Snyder, *Materials Today Physics*, 2018, **6**, 83-88.
2. C. G. Maier and K. Kelley, *Journal of the American chemical society*, 1932, **54**, 3243-3246.
3. M. Paliwal and I.-H. Jung, *Calphad*, 2009, **33**, 744-754.